Available online at www.sciencedirect.com
ScienceDirect
Food Chemistry 102 (2007) 454–465
Food Chemistry
www.elsevier.com/locate/foodchem

Development of an on-line optical method for assessment of the bubble size and morphology in aerated food products

Mohsen Labbafi [a,b], Rajeev K. Thakur [a], Christophe Vial [a], Gholamreza Djelveh [a,*]

[a] LGCB, Université Blaise Pascal, 24 avenue des Landais, BP 206, F-63174 Aubière Cedex, France
[b] Department of Food Technology, University of Tehran, Iran

Abstract

The quality of whipped products of the food industry is closely linked to the characteristics of the dispersed gas phase, such as the bubble morphology, the mean bubble size and the uniformity of the bubble size distribution. Here, an on-line method based on imaging techniques was developed for measuring these quantities in food foams manufactured in a continuous foaming device. On-line image acquisition was based on a quartz visualization cell that ensured a continuous renewal of the samples. The mean bubble size and the bubble size distribution were obtained using a semi-automated image analysis procedure. The method was validated on four kinds of aerated food emulsions (ice cream, whipped cream, aerated fresh cheese and a foamed sauce), corresponding to a large range of overrun (30–180%). The σ/d_{32} ratio of bubble size distributions of dairy foamed emulsions was shown to be nearly constant, regardless of the recipe and of operating conditions.

Keywords: Bubble; Food foam; Aerated food; On-line method; Whipping process

1. Introduction

Many food products correspond to aerated foods, such as baked products, extruded and expanded cereal products, egg products, confectionaries, dairy products and a class including foams based on meat, fish, vegetable or fruits (Campbell & Mougeot, 1999). Up to the early nineties, only the contributions of ingredients on aerated food microstructure were emphasized in the literature (see, e.g., Stanley, Goff, & Smith, 1996, for ice cream and whipped cream). Conversely, the role of bubbles as ingredients in food systems was disregarded. This is one of the main reasons that explain why aerated foods are still less understood than other food systems. However, the situation has changed since the late eighties when food processors have ''rediscovered'' the opportunity to use a gas phase as a zero-cost ingredient in order to manufacture innovative products. Indeed, including a gas phase into a continuous medium in form of tiny bubbles not only affects texture and firmness, making the product lighter, but also appearance, colour and mouth-feel (Campbell, Webb, Pandiella, & Niranjan, 1999). This may confer sensory and marketing advantages to aerated foods over conventional products, such as softness and scoopability, a more uniform distribution of flavours and an enhanced homogeneity.

As a result, aeration has become one of the fastest growing processing operations in the food industry in the nineties (Campbell et al., 1999) and it could be considered as a simple way of innovation in traditional food. This is particularly true for aerated foods in which an external gas phase is dispersed into a continuous matrix through mechanical action denoted mixing, whipping, shaking or foaming. In this particular case, there is however a strong interplay between the recipe of the raw material, the technologies involved and the operating conditions of gas dispersion (see, e.g., Labbafi, Vial, & Djelveh, 2005). Although the interest of food processors for aeration has levelled off

* Corresponding author. Tel.: +33 4 73 40 50 55; fax: +33 4 73 40 78 29.
E-mail address: djelveh@univ-bpclermont.fr (G. Djelveh).

0308-8146/$ - see front matter © 2006 Elsevier Ltd. All rights reserved.
doi:10.1016/j.foodchem.2006.06.011

Nomenclature

d	diameter (m)
d_i	diameter of ith object (m)
d_{ij}	average diameter calculated using Eq. (3) (m)
G	liquid flow rate (m^3/s)
i, j, k	integers (–)
L	gas flow rate (m^3/s)
n	sample size (–)
N	rotation speed (s^{-1})
S	object surface area (m^2)

Greek letters

Φ	overrun
Φ_{max}	maximum overrun under steady state conditions (–)
σ	standard deviation of the bubble size distribution (m)
σ_m	standard deviation of d_{32} between images (m)

since the end of the nineties, there is still much to understand on the role of bubbles as food ingredients and the interactions between formulation and process in aerated foods.

The main difficulty that has limited the introduction of gas phase as an ingredient in traditional food is the lack of reproducibility often observed in the manufacturing of aerated foods. Indeed, the gas content and the size distribution of the gas cells are the key parameters that govern the properties of aerated foods are difficult to control. This is particularly the case in batch whipping operation: for example, the relations between the recipe, the quality of the gas dispersion and the whipping time are complex, as this has been illustrated by Brooker, Anderson, and Andrews (1986) and Van Aken (2001) for whipped cream or Massey, Khare, and Niranjan (2001) for cake batter. The quality of aerated foods in terms of texture and stability could generally not be guaranteed in this case. To circumvent this problem, food processors have often preferred continuous whipping operation under steady state conditions, generally using scraped surface heat exchangers (Gonzáles Méndez, 1990) or rotor–stator devices (Müller-Fischer & Windhab, 2005): constant flow rates, residence time and mixing conditions over time should ensure reproducible properties. However, the limitations of continuous whipping and especially the occurrence of an oscillating regime have been pointed out by Kikuchi, Endo, Yoshioka, Watanabe, and Matsumoto (1995). As a conclusion, even in the continuous process, the establishment of methods for the assessment of gas dispersion during and after aeration is still needed, which implies reliable measurements of both the gas content and the way the gas is spatially distributed.

While the gas content is usually described in the literature using density, specific volume or overrun (which corresponds to the volume of gas per volume of gas-free material), information on bubble size distribution is scarce, although bubble size is known to act both on the mechanical properties and the stability of the foams and it may also contribute to the changes in appearance (German, 1990; Stanley et al., 1996). The main reason is that the microscopic properties of individual bubbles are more difficult to measure than the macroscopic properties of aerated foods. As imaging techniques based on optical microscopy constitute the most widespread way to analyze bubble size distribution in the food industry, this situation stems mainly from the opacity of semi-solid and solid aerated foods and from the fragility of low and intermediate viscosity foams. For example, opacity and fragility induce the application of image pre-treatments, including sampling, eventually followed by sample pressing, slicing or fracturing. These may therefore lead to biased information.

Imaging techniques can be divided into three steps: image acquisition, object detection and morphology measurements, the last two being strongly dependent on the image acquisition procedure (Fig. 1). While the limitations of bubble morphology measurements have been widely discussed in the literature (Kroezen & Groot Wassink, 1987), the influence of sample preparation has been hardly ever addressed. The five main drawbacks of these pre-treatments on object detection can be summarized as follows:

(1) The method used for sampling and the position of the sample may considerably affect the bubble morphology, the spatial distribution of the bubbles and therefore the procedure used for contour detection.
(2) The thickness of the samples is generally not uniform and too large for direct observation. The non-uniformity induces light intensity gradients in the images, while thick samples increase the probability to measure bubbles located in different layers. On the other hand, the methods to make samples thinner and more uniform may alter the structure of the foam.
(3) The structure of the foams may be sensitive to heat and may change rapidly due to the microscope light source if the samples are not cooled.
(4) The contrast between the bubbles and the background is generally poor.
(5) For aerated food emulsions, when the bubble-to-fat globule diameter ratio is low or when multilayer adsorption occurs, adsorbed fat droplets make the air/water interfaces irregular, even when the bubbles are spherical.

Several solutions that can circumvent one or several of these drawbacks have been described in the literature.

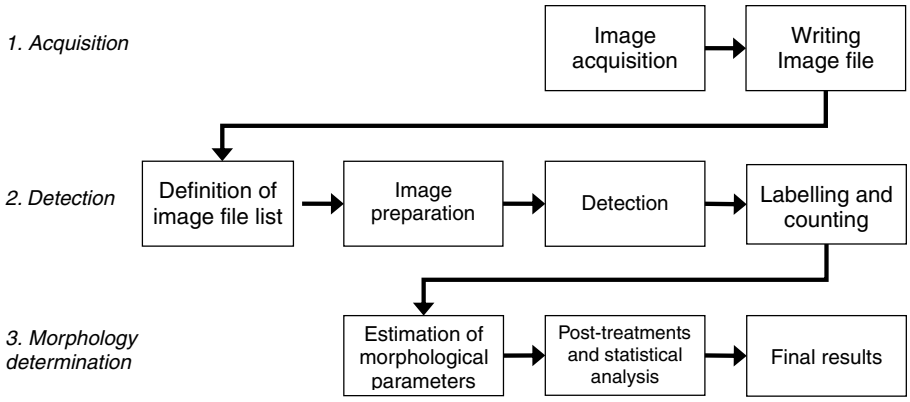

Fig. 1. Schematic description of image analysis procedures.

Chang and Hartel (2002) used a depression slide to standardize sample thickness. A cell of 50 μm thickness formed by two microscope slides was used by Sahi and Alava (2003). A similar 250 μm system was used by Massey et al. (2001). Although powerful image analysis software packages are available now, the consequence of the limitations listed above is that manual measurements or manual reconstruction of bubble contours are still applied (see, e.g., Lim & Barigou, 2004), which limits the statistical validity of reconstructed bubble size distribution.

The objective of this work is therefore to establish a reliable method to characterise bubble size and morphology in aerated food manufactured using a continuous foaming device. This includes the development of an on-line microscopic image acquisition technique that is versatile enough to be used in a wide range of operating conditions and gas content, but also of an adapted procedure able to measure nearly automatically the morphological parameters of the bubbles. Both should contribute to improve the speed, the reproducibility and the reliability of bubble size measurements in foams. These should finally provide a tool that will be able to assess the quality of whipped products during continuous whipping in aeration lines of the food industry. Several applications illustrating the potentiality of this tool will be reported.

2. Experimental

Four raw materials, namely, a model emulsion with the typical composition of a white sauce, a commercial fresh cheese in which stabilizers (pectin, carrageenan or xanthan) have been added to enhance foam stability and two industrial dairy mixes corresponding respectively to typical recipes of ice cream and whipped cream were subjected to continuous aeration in order to validate the applicability of the imaging technique. They correspond to food emulsions, which makes usually object detection more difficult. The recipes of these four products are summarized in Table 1. Except for the fresh cheese, the pH values are close to neutrality and pH is far higher from the isoelectric point of proteins. Continuous aeration was carried out in a laboratory-scale mechanically stirred column described in previous works (Thakur, Vial, & Djelveh, 2003). The impeller speed in the column could be controlled between 200 and 1200 rpm; gas and liquid volumetric flow rates at the bottom of the column could be adjusted between 10 and 30 mL/min using a mass flowmeter and a peristaltic pump respectively. Flow rates were chosen in order to manufacture a 100% overrun foamed white sauce (Thakur et al., 2003), a 100% overrun ice cream (Thakur, Vial, & Djelveh, 2005), a 180% overrun whipped cream and a 30% overrun fresh cheese (Vial, Thakur, Djelveh, & Picgirard, 2006; Vial, Thakur, Pérez Quintáns, Djelveh, & Picgirard, 2006), using the fact that the maximum overrun Φ_{max}, when the Laplace pressure in the bubbles is neglected, is expressed as

$$\Phi_{max} = \frac{G}{L} \quad (1)$$

These values were retained in order to fit commercial products. Using the circulation of a coolant in the jacket, the draw temperatures of the aerated materials were maintained at 4 °C for the foamed white sauce, the aerated fresh cheese and whipped cream, while it was −2 °C for ice cream, which is just above the freezing point of this emulsion. The equipment available for bubble size measurements consisted of an inverted phase-contrast microscope (Axiovert-25, Carl Zeiss Jena GmbH, Germany), a CCD camera (Kappa Opto-Electronics GmbH, Germany) and

Table 1
Composition and pH of the four raw materials

Raw material	Composition (%w/w)			
	White sauce	Ice cream mix	Whipped cream mix	Fresh cheese
Fat	15.0	9.0	20.0	8.0
Proteins	4.0	3.0	6.5	6.8
Sucrose/lactose	–	17.0	15.0	3.8
Starch	6.0	–	–	–
Other gums	0.5	0.2	0.25	0.1–0.25
Emulsifiers	–	0.3	0.25	–
Others (salts...)	1.0	–	–	1.2
pH	6.6	6.7	6.7	5.0

an image analysis software package that could be used both for image acquisition and analysis (ImagePro+ 4.01 from MediaCybernetics, MD, USA).

3. Results and discussion

3.1. Development of the image acquisition method

The objective was to find a method able to maintain a constant sample thickness and could be applied in a large range of flow rates and overrun, but avoided simultaneously mechanical treatments and rapid pressure or temperature changes. The solution retained consisted of an on-line method based on a quartz visualization cell kept underneath the phase contrast microscope. This cell was placed on a sampling flow line located on the exit stream of the column (Fig. 2). The inlet and the outlet region of the cell were designed with a V shape to avoid a sudden change in foam velocity. A valve was used to control the flow rate in the sampling line, which ensured a continuous renewal of the foam in the visualization cell, while maintaining foam velocity low enough to avoid any axial bubble deformation due to flow conditions. The valve position and the geometry of the cell were also adjusted to slow down the bubbles in the camera field of view. The rectangular cell thickness was 2 mm, as this value was about 10 times higher than the estimated maximum size of the bubbles in the food foams studied. Image acquisition on 2 mm thickness samples was possible only owing to the use of an inverted phase contrast microscope: phase contrast microscopy is a type of light microscopy that enhances contrasts of transparent and colourless thick objects by influencing the optical path of light, which improves the quality of foam images and make the bubbles "inside" the sample more visible than those in the foreground. The maximum width of the visualization cell was 2.5 cm in order to maintain the ratio between the velocity in the sampling line and the velocity in the cell lower than 2. As a result, the mechanical treatments applied to the samples were minimized and the influence of pressure and temperature changes during sampling became negligible compared to a manual sampling procedure. Another advantage of the on-line image acquisition method developed above is the possibility of full automation by controlling the image capture frequency, using the camera control software or the macros of the image acquisition software, once the valve and the microscope light intensity were adjusted. Finally, 640×515 images in 256 grey-level uncompressed TIF format could be saved for further analysis. This gave access to a large amount of data illustrated by Fig. 3 that could be useful for statistical purpose. This amount of data is however useless unless a semi-automated image analysis method is developed.

3.2. Development of the image analysis procedure

The main difficulties in the development of an automated image analysis procedure reported in Section 1 appear clearly in Fig. 3: the contrast between the background and the bubbles is weak and only bubble interfaces appear as "dark"; the background is not uniform and there are black areas in the corners, the bubble–bubble distance is low and touching bubbles can be seen. However, the images show that the bubbles can be assumed to be roughly spherical, as they appear as irregular circles in the photos. As a result, the only morphological parameter of interest is the equivalent circle diameter. The simplest methods that can be used for the treatment of the images of Fig. 3 are the following: one can either detect dark objects, corresponding to the interfaces, or bright objects corresponding to bubble interior. Image preparation can therefore be defined as follows (Fig. 4):

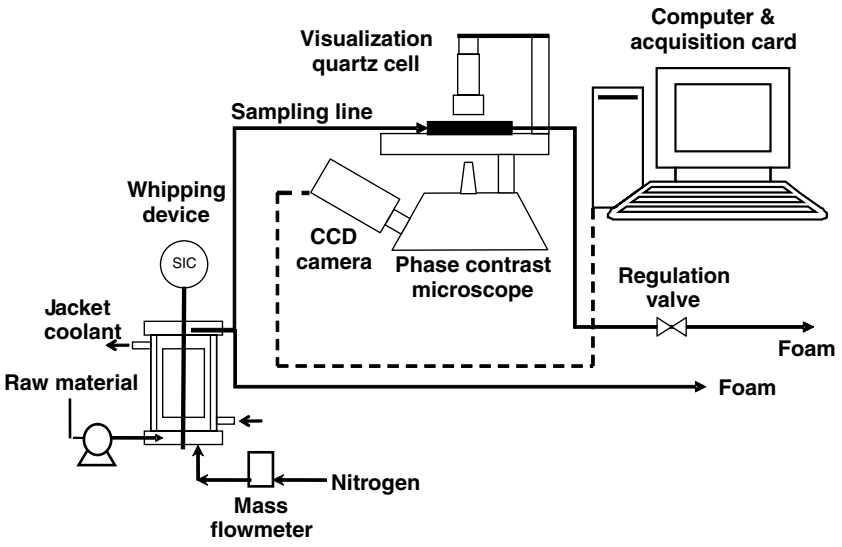

Fig. 2. Schematic description of the on-line image acquisition procedure.

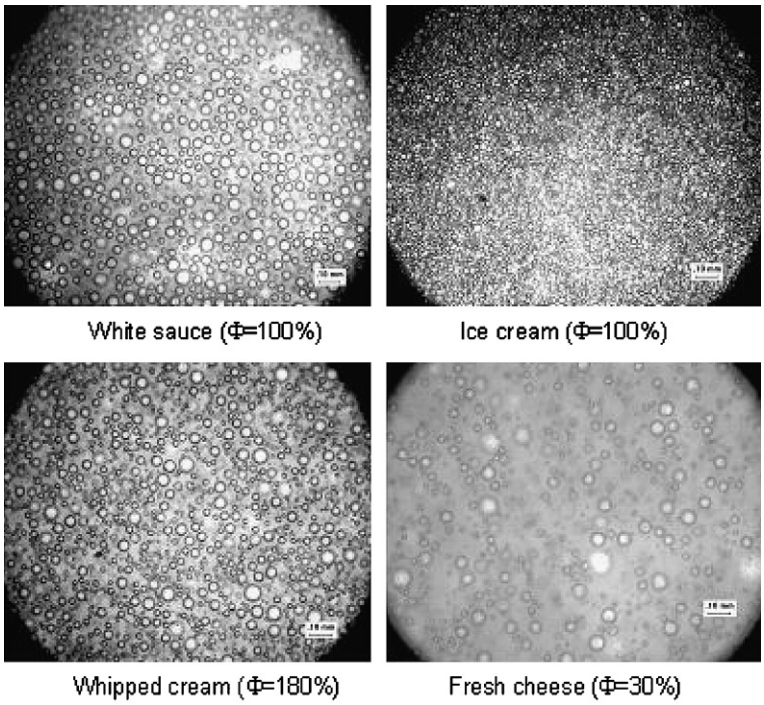

Fig. 3. Examples of images acquired using the on-line procedure.

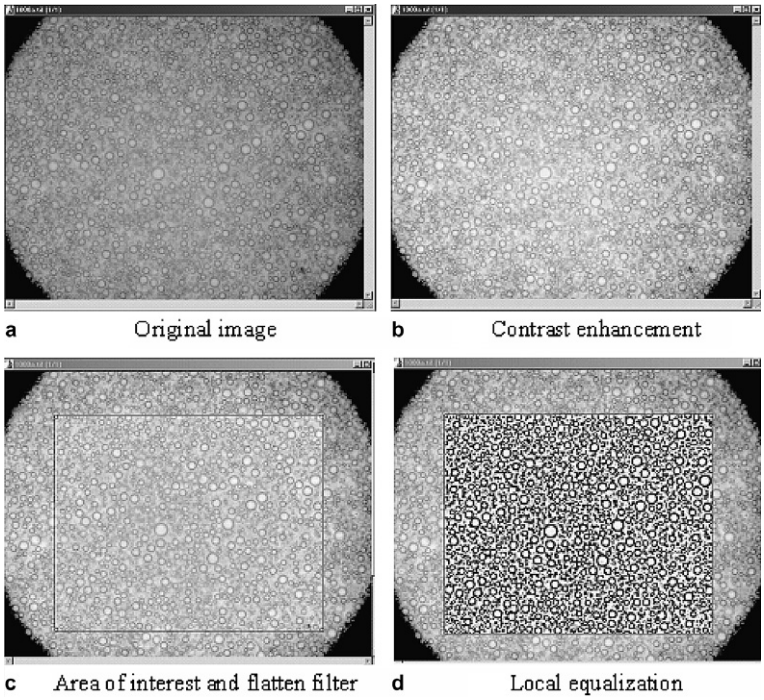

Fig. 4. Example of image preparation for bubble detection.

(1) Contrast enhancement for enlarging the light intensity histogram (Fig. 4b).
(2) The definition of a zone of interest excluding the dark corners of the images (Fig. 4c).
(3) *Flatten filter* for evening out background variations in pixel intensity in the area of interest (Fig. 4c); a more uniform background is therefore obtained.
(4) *Local equalization* to enhance bubble interfaces by increasing pixel contrast based on the histogram of the local neighbourhood. The histogram is then equally distributed across the intensity scale, which produces a high contrast image with the highest possible dynamic range (Fig. 4d).The image in Fig. 4d can sometimes be used directly for the detection of

bright objects, as the problems induced by light intensity gradients, poor contrast, irregular interfaces and touching bubbles have been solved. However, additional image pre-treatments can still improve image quality, especially when the objective is dark object detection, such as

(5) The application of the *median filter* to remove impulse noise and close the interfaces, while preserving the edges and contours (Fig. 5b).

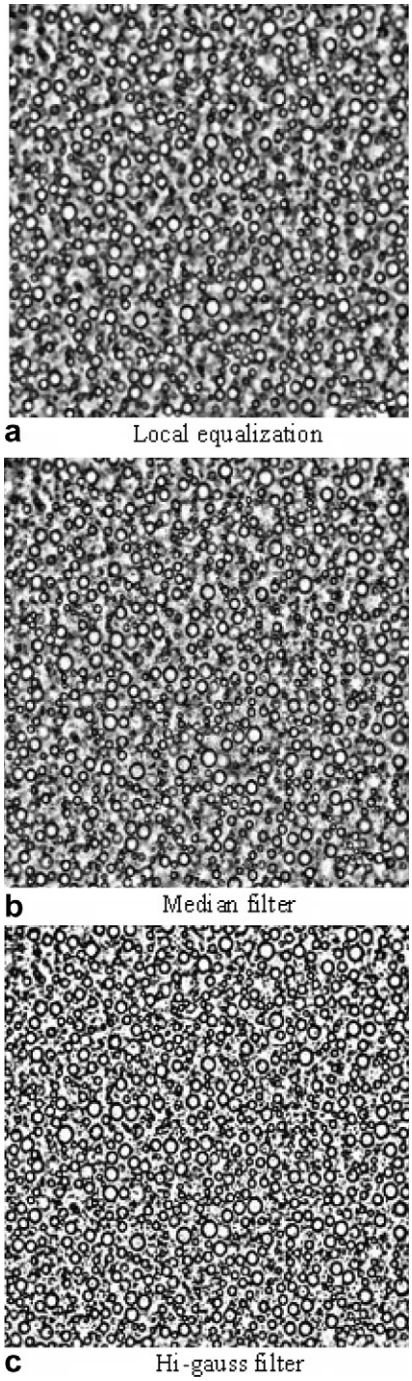

Fig. 5. Example of final enhancement of the images before detection.

(6) The enhancement of the fine details of the interfaces using the *hi-gauss filter*, which is a high-pass filter that eliminates low frequency using a Gauss function (Fig. 5c).

The adjustable parameters in the six steps described above are mainly the kernel size of the median and hi-gauss filters and the number of times these filters are applied successively.

Using the standard procedures of ImagePro+, a semi-automatic detection of bright objects was generally preferred, while detection of dark objects was equivalent only when the number of touching bubbles was low. Manual operations include only the definition of the image list (Fig. 1) and that of the adjustable parameters cited above. This method was based on image segmentation using thresholding on the basis of pixel intensity in the histogram of the intensity characteristics of the image. The detection procedure was followed by automatic counting and labelling of the objects. Morphological parameters reported for each object include the diameter d_i, considering that the bubbles are spherical

$$d_i = \sqrt{\frac{4S}{\pi}} \tag{2}$$

where S is the surface area of the ith object. The other interesting features provided by the software include the *elongation* or *aspect ratio*, which is a measurement of the width/length relationship and has values in the range 0–1, and the *circularity* which is a measurement of the ratio of the actual perimeter of a particle to the perimeter of a circle with the same area. Circularity is a measurement of irregularity or difference from a perfect circle and has also values in the range 0–1 (a perfect circle has a circularity of 1, while a very spiky or irregular object has circularity closer to 0). Elongation and circularity can be used in post-treatments (Fig. 1) to filter undesirable objects. Post-treatments are generally reduced to the definition of the minimum size of an object when the detection of bright objects is applied. Conversely, when the detection of closed dark objects is used, elongation and circularity criteria have to be used to discard touching bubbles and other dark objects in the background (see, e.g., Fig. 5).

Statistical analysis includes the sample size n (number of bubbles detected) and the average diameters d_{ij} ($0 \leqslant j < i$) defined as

$$d_{ij} = \left(\frac{\sum_{k=1}^{n} d_k^{i+1}}{\sum_{k=1}^{n} d_k^{j+1}} \right)^{\frac{1}{i-j}} \tag{3}$$

A correction to Eq. (3) has been described by Kroezen and Groot Wassink (1987) to take into account the relation between the bubble size and the ease of detection. These authors considered that the d_{ij} of the raw bubble size distribution was equal to the $d_{i+1,j+1}$ of the true size distribution because large bubbles are more easily detected. This correction is however not general (Chang & Hartel, 2002). In this

work, the Sauter diameter d_{32} was finally retained for further analysis, which is a compromise between the two methods: it corresponds to the surface-average diameter of the uncorrected distribution and the volume-average diameter when the correction is applied. Other descriptors are the standard deviation σ of the raw distribution, which estimates the width of the bubble size distribution, and the standard deviation of d_{32} between several images σ_m, which is a measure of the error on d_{32} estimation. The macro language of the software was used for automating image analysis and the reporting of the results.

3.3. Validation of the image analysis procedure

In order to assess the validity of the image analysis procedure, four aerated emulsions corresponding to overrun values between 30% and 180% have been studied. The influence of operating conditions on bubble size has also been considered, such as rotation speed N for whipped cream, ice cream and the white sauce, or residence time τ for ice cream and whipped cream. First, the definition of the minimum sample size n for bubble diameter estimation has been investigated. In the literature, this remains an open question: Kroezen and Groot Wassink (1987) and Chang and Hartel (2002) counted 250 bubbles, Hanselmann and Windhab (1999) counted 300 bubbles, Thakur et al. (2003) analyzed a minimum of 500 bubbles, while Allais, Edoura-Gaena, Gros, and Trystram (2006) counted about 600 bubbles. The same question stands for the number of images, which is almost never discussed, except for example by Allais et al. (2006) that used three images per set of operating conditions. In this work, five images were taken in each set of operating conditions in order to estimate σ_m. Sample size varied as a function of overrun and d_{32} from an average of 500 bubbles in the aerated fresh cheese to more than 1500 in unfrozen ice cream. The validation of sample size consisted of the calculation of "moving" $d_{10}(k)$ and $\sigma(k)$ values with $1 < k \leqslant n$:

$$d_{10}(k) = \frac{1}{k}\sum_{i=1}^{i=k} d_i; \quad \sigma(k) = \left[\frac{1}{k-1}\sum_{i=1}^{i=k}(d_i - d_{10})^2\right]^{1/2} \tag{4}$$

These parameters are illustrated for ice cream and fresh cheese in Fig. 6. This figure shows that d_{32} and σ became nearly constant when n was higher than 300, which means that a sample size between 500 and 600 bubbles was usually high enough for d_{32} and σ estimation, in agreement with the literature.

For comparison and validation, the automatic analysis procedure was compared to manual image analysis. This manual method was based on the possibility offered by the software to define manually circular objects by clicking on three points of their borders (Thakur et al., 2003). Sample size n, d_{32} and σ were compared on the same set of images for the four raw materials. The results showed that both methods agreed, as this is illustrated in Fig. 7 for ice cream at different rotation speed, as ice cream corresponds to the case of where many touching bubbles are observed. The difference in d_{32} values on five images was generally below 2 μm (Fig. 7a), while the difference in n values was always lower than 10% and often lower than 5% (Fig. 7b). Manually measured d_{32} values were usually a bit higher because the automatic method measured bright objects, while the circle included in general the dark interface. However, this effect was sometimes counterbalanced by the irregular shape of the bubbles that was not taken into account by circles. The difference in n values stems mainly from bubbles that were assumed to be in the back-

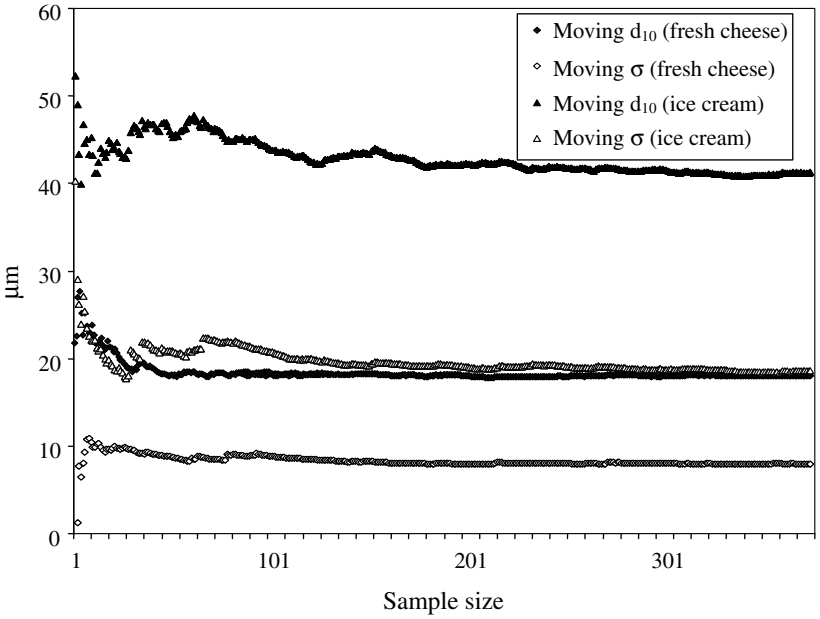

Fig. 6. Example of the evolution of moving d_{32} and σ values for ice cream and fresh cheese samples.

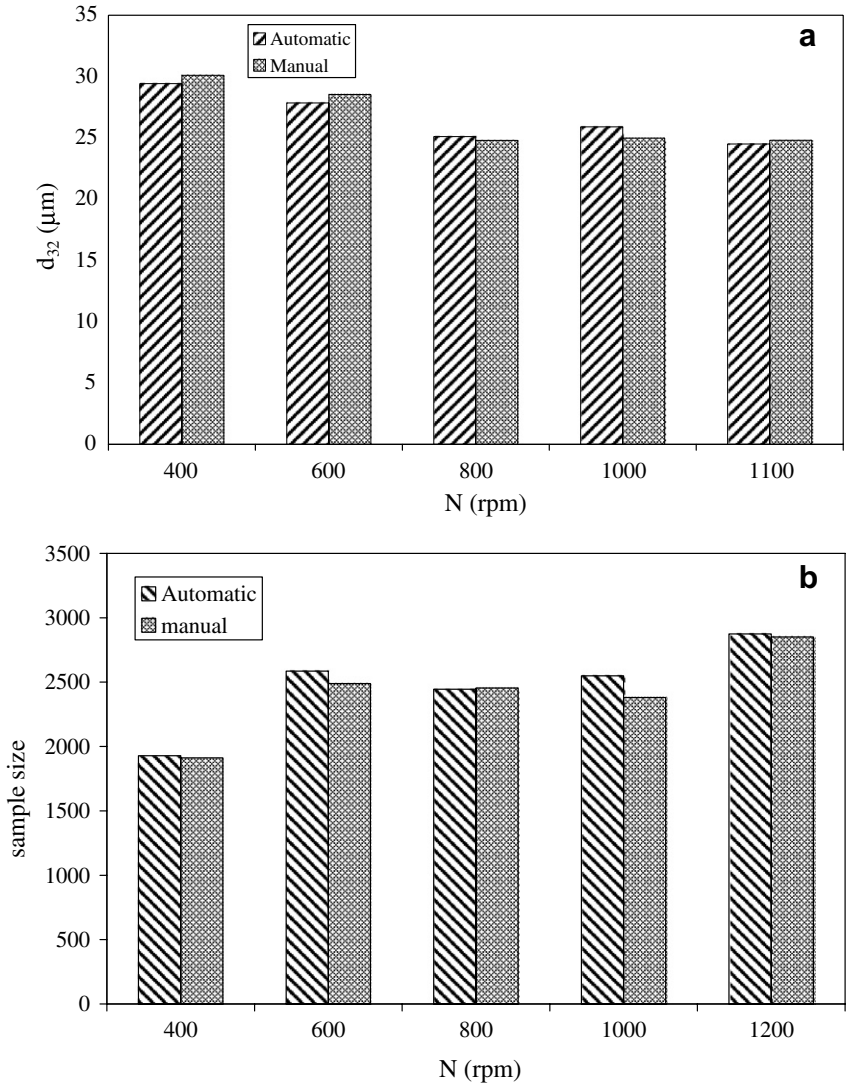

Fig. 7. Comparison of d_{32} and n values from manual and automatic analysis on ice cream samples obtained at different rotation speed N.

ground by the user, but were sometimes counted by the automatic procedure. As a result, the difference between manual and automatic procedures is close to that estimated between the detection of bright and dark objects, which was around 1 μm when all the touching bubbles were removed from the samples by elongation and circularity criteria for dark object detection.

The interest of an automated image acquisition procedure appears clearly when σ_m is taken into account. Fig. 8 illustrates the influence of rotation speed N on σ_m. This shows that σ_m decreased significantly from about 2.5 to 0.5 μm when rotation speed was increased. A σ_m value of 2 μm between five images represented a ratio around 8%, which seemed however high for ice cream samples if one considers that the sample size per image was between 400 and 500 bubbles. Additionally, σ_m/d_{32} followed the same trends as σ_m as a function of rotation speed and this ratio decreased also when the number of images was increased. This is in agreement with the literature, as Allais et al. (2006) found σ_m/d_{32} around 15% for three images of aerated cake batter, while it was always lower than 10% for five images in this work, regardless of overrun and operating conditions. This means that the error on d_{32} estimation can be reduced for all the raw materials by increasing significantly the number of images, using the automated image acquisition procedure that can provide and analyze automatically a large set of pictures.

As a conclusion, the interest of the on-line image acquisition technique has been confirmed and the semi-automatic image analysis method has been validated, as the statistical parameters obtained are close to those of the manual method. The applicability of the whole procedure has been demonstrated for the four raw materials (overrun between 30% and 180%) and particularly for ice cream images that exhibit many touching bubbles. Therefore, automation of image capture and analysis can potentially improve the accuracy of d_{32} and σ estimation. On the other hand, the deviation of d_{32} values between successive

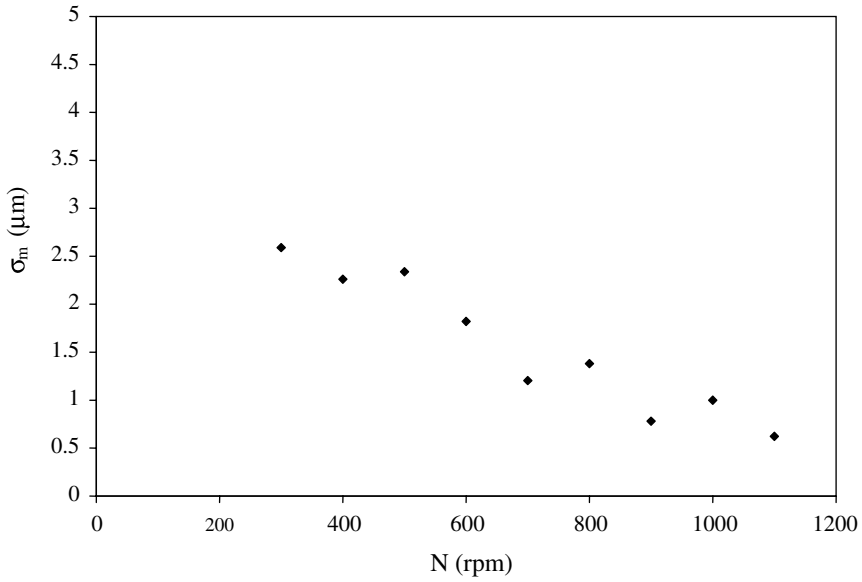

Fig. 8. Illustration of the evolution of σ_m as a function of rotation speed N for ice cream.

images, especially with whipped cream, can be used to characterize unstable or oscillating conditions. Although the image treatments applied are still time-consuming, one can consider roughly that the automated procedure is about 10 times quicker than a full manual treatment.

3.4. Application to the analysis of the influence of process parameters

Experimental data obtained with the foamed white sauce and unfrozen ice cream confirms previous results (Thakur et al., 2003, 2005). These results will not be detailed and one will only remind that d_{32} decreased when N and τ increased for both products, with d_{32} values usually between 30 and 50 µm for aerated white sauce and 15–35 µm for unfrozen ice cream respectively. Similar trends were observed for σ values. For whipped cream, "overwhipping" had often been reported in the literature (Brooker et al., 1986; Van Aken, 2001). This phenomenon corresponds to a decrease in overrun generally observed when rotation speed is too high or whipping time is too long. Obviously, similar results were observed during the continuous manufacturing of whipped cream, as this can be seen in Fig. 9: when the residence time was low, the d_{32} and σ curves passed simultaneously through a minimum around 1000 rpm; when the residence time was high, d_{32} remained high and nearly constant. Conversely, it is probable that overwhipping was delayed to higher rotation speed because draw temperature was low in the case of ice cream and because of the high stabilizer content in the case

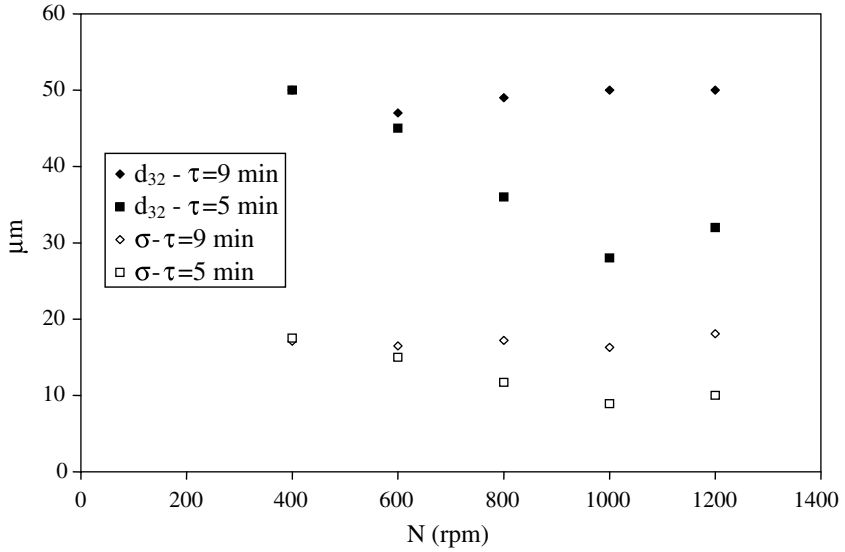

Fig. 9. Evolution of d_{32} and σ values for whipped cream as a function of rotation speed and residence time.

of the foamed white sauce. For aerated fresh cheese, the evolution of overrun with operating conditions was so high that an analysis based only on d_{32} and on the bubble size distribution was inadequate (see, e.g., Vial, Thakur, Djelveh et al., 2006; Vial, Thakur, Pérez Quintáns et al., 2006).

As a conclusion, the image analysis method developed in this work has been able to estimate the influence of operating conditions for three aerated foods and to highlight overwhipping in the case of whipped cream. The results demonstrate therefore the potential applicability of the image analysis technique to assess the quality of whipped products and to optimize the operating conditions of continuous foaming operation, using d_{32} and σ as criteria.

3.5. Application to the comparison of whipped products properties

In Section 3.4, it was reported that the image analysis method could be used in order to compare the four aerated foods. The typical cumulated bubble distributions of these four products are reported in Fig. 10. All were monomodal, regardless of the raw materials and the same stands for operating conditions when overrun was close to the maximum value given by Eq. (1). This is in agreement with the literature (Kroezen & Groot Wassink, 1987; Chang & Hartel, 2002; Allais et al., 2006). For nearly similar operating conditions, one has generally d_{32} (ice cream) $< d_{32}$ (white sauce) $< d_{32}$ (fresh cheese). This is illustrated for example in Fig. 3 in which d_{32} (ice cream) $= 15$ μm, d_{32} (white sauce) $= 44$ μm and d_{32} (fresh cheese) $= 52$ μm. The situation is more complex for whipped cream because this emulsion was far more sensitive to operating conditions. For example, d_{32} (whipped cream) $= 37$ μm in Fig. 3, but d_{32} values between 30 and 130 μm were also reported. Although the bubble size distributions seem very different in Fig. 9, those of the three dairy products presented surprisingly constant features. Fig. 11 represents the evolution of σ as a function of d_{32} for all the recipes, combining all the operating conditions used in this work. For the three dairy emulsions, σ and d_{32} were shown to be related by a power-law relation in which the exponent is close to 1, although overrun varied from 30% for the fresh cheese to 180% for whipped cream and the pH of fresh cheese was close to the isoelectric point of caseins and whey proteins. In this case, the σ/d_{32} ratio was about 0.33 ± 0.02. Only the aerated white sauce presented a lower σ for a constant d_{32} value, which means that the bubble size distributions of the three dairy emulsions were wider for the same average diameter. This is probably linked to the composition of the three dairy foods that contained exactly the same ingredients, but with different proportions, while a large amount of starch was added in the white sauce. For dairy emulsions, the recipe and the foaming temperature affect widely the rheological properties of the mixes (see, e.g., Thakur et al., 2005 & Vial, Thakur, Pérez Quintáns et al., 2006), acting therefore on d_{32}, but the recipes of the three dairy emulsions studied in this work contained the same amount of stabilizers and milk proteins were always in excess. Consequently, the mechanisms of bubble stabilization were nearly the same: bubbles were mainly stabilized by the combined adsorption of proteins and fat globules, which was reinforced by the minute addition of stabilizers (see, e.g., Stanley et al., 1996; Van Aken, 2001). Conversely, the aerated white sauce was mainly stabilized by starch and the high viscosity of the continuous phase (Thakur et al., 2003; Mandala, Savvas, & Kostaropoulos, 2004). This prevented probably recoalescence and reduced therefore the width of bubble size distributions, although further work is required to confirm this assumption. For example, one could check whether aerated white sauce follows the same kind of power-law between σ and d_{32} by varying the composition of the sauce, as the d_{32} range is too short with the composition and the range of operating conditions studied in this work. However, this

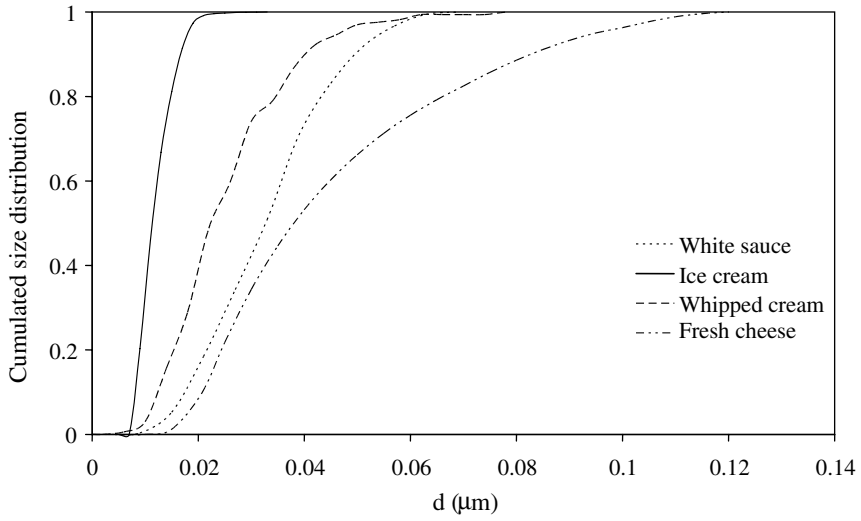

Fig. 10. Example of cumulated bubble size distribution for the four aerated foods.

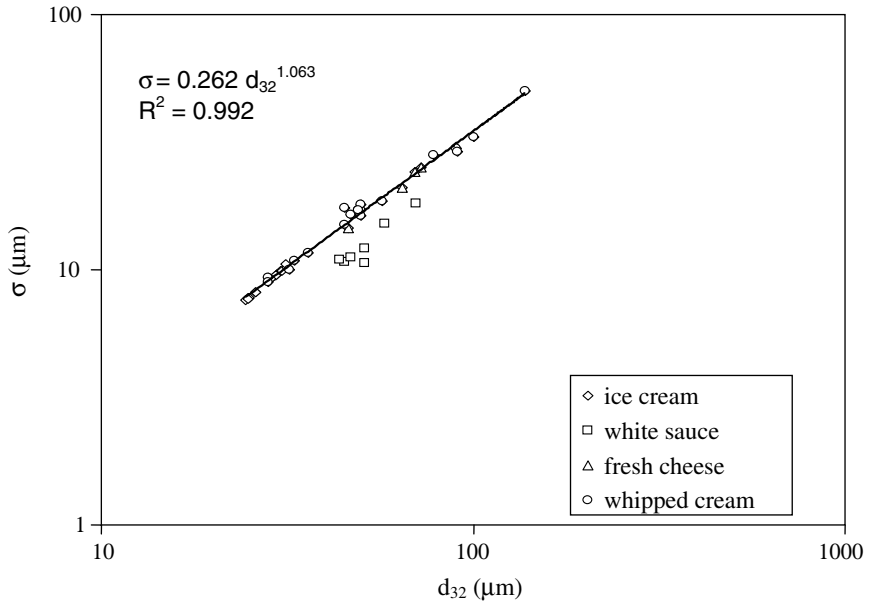

Fig. 11. Evolution of σ as a function of d_{32} for the four types of aerated foods, regardless of operating conditions.

is likely to occur, as one found $\sigma/d_{32} \approx 0.25 \pm 0.03$ for the white sauce in this work and also because Kroezen and Groot Wassink (1987) had already found a similar relationship for aqueous foams thickened by starch for use in textile technology.

As a conclusion, the on-line image acquisition method and the automatic image analysis procedure have been applied successfully for the determination of constant features in the bubble size distributions of dairy aerated foods, regardless of overrun and operating conditions. The results have also highlighted the role of stabilizers on the bubble size distribution of foamed foods. This provides interesting perspectives for further research on the interactions between formulation, technology and operating conditions in order to improve the quality of whipped products manufactured using continuous process.

4. Conclusions

In this work, an on-line image acquisition technique and a semi-automatic image analysis procedure have been validated for the analysis of bubbles in aerated foods manufactured using continuous foaming operation, covering a 30–180% range in terms of overrun and a 10–130 μm range in terms of Sauter diameter. The on-line optical method developed in this work constitutes therefore a useful tool to assess the quality of whipped products, but also a versatile tool for investigating the effect of the interactions between formulation, technology and operating conditions on the properties of aerated foods. As the additional costs induced by the on-line method include only the design, scale-up and construction of the by-pass and the visualization cell, the perspectives involve mainly the design and development of control algorithms for improving the continuous manufacturing of aerated food products using the on-line image analysis technique.

References

Allais, I., Edoura-Gaena, R.-B., Gros, J.-B., & Trystram, G. (2006). Influence of egg type, pressure and mode of incorporation on density and bubble distribution of a lady finger batter. *Journal of Food Engineering, 74*, 198–210.

Brooker, B. E., Anderson, M., & Andrews, A. T. (1986). The development of structure in whipped cream. *Food Microstructure, 5*, 277–285.

Campbell, G. M., & Mougeot, E. (1999). Creation and characterisation of aerated food products. *Trends in Food Science & Technology, 10*, 283–296.

Campbell, G. M., Webb, C., Pandiella, S. S., & Niranjan, K. (1999). *Bubbles in food*. St Paul, MN, USA: Eagan Press.

Chang, Y., & Hartel, R. W. (2002). Measurement of air cell distributions in dairy foams. *International Dairy Journal, 12*, 463–472.

German, J. B. (1990). Properties of stabilising components in foams. In *Food emulsion and foam: theory and practice*. In P. J. Wan, J. L. Cavallo, F. Z. Saleeb, & M. J. McCarthy (Eds.). *AIChE Symposium Series* (Vol. 86, pp. 62–70). New York: AIChE.

Gonzáles Méndez, N. F. (1990). Mise en oeuvre d'un procédé de foisonnement en continu en échangeurs de chaleur à surface raclée. Elaboration de mousses de viande et de poisson. PhD Thesis. Aubière (France): Université Blaise Pascal.

Hanselmann, W., & Windhab, E. J. (1999). Flow characteristics and modelling of foam generation in a continuous rotor/stator mixer. *Journal of Food Engineering, 38*, 393–405.

Kikuchi, M., Endo, M., Yoshioka, T., Watanabe, R., & Matsumoto, S. (1995). Modelling and dynamic analysis of a continuous whipping system. *Milchwissenschaft, 50*, 129–134.

Kroezen, A. B. J., & Groot Wassink, J. (1987). Bubble size distribution and energy dissipation in foam mixers. *Journal of the Society of Dyers and Colourists, 103*, 386–394.

Labbafi, M., Vial, Ch., & Djelveh, G. (2005). Influence of pH and pressure homogenization on the continuous foaming process applied to dairy fermented foods. In C. Larroche, A. Pandey, & C. G. Dussap (Eds.), *Current topics in bioprocess in food industry* (pp. 235–249). New Delhi, India: Asiatech Pub. Inc.

Lim, K. S., & Barigou, M. (2004). The effects of high intensity ultrasound on foam structure. In *Proceedings of the 9th International Congress on Engineering & Food (ICFEF9)* Montpellier (France), pp. 597–602.

Mandala, I. G., Savvas, T. P., & Kostaropoulos, A. E. (2004). Xanthan and locust bean gum influence on the rheology and structure of a white model-sauce. *Journal of Food Engineering, 64*, 335–342.

Massey, A. H., Khare, A. S., & Niranjan, K. (2001). Air inclusion into a model cake batter using a pressure whisk: development of gas hold-up and bubble size distribution. *Journal of Food Science, 66*, 1152–1157.

Müller-Fischer, N., & Windhab, E. J. (2005). Influence of process parameters on microstructure of food foam whipped in a rotor–stator device within a wide static pressure range. *Colloids and Surfaces A: Physicochemical and Engineering Aspects, 263*, 353–362.

Sahi, S. S., & Alava, J. M. (2003). Functionality of emulsifiers in sponge cake production. *Journal of the Science of Food and Agriculture, 83*, 1419–1429.

Stanley, W., Goff, H. D., & Smith, A. K. (1996). Texture–structure relationships in foamed dairy emulsions. *Food Research International, 29*, 1–13.

Thakur, R. K., Vial, Ch., & Djelveh, G. (2003). Influence of operating conditions and impeller design on the continuous manufacturing of food foams. *Journal of Food Engineering, 60*, 9–20.

Thakur, R. K., Vial, Ch., & Djelveh, G. (2005). Combined effects of process parameters and composition on foaming of dairy emulsions at low temperature in an agitated column. *Journal of Food Engineering, 38*, 335–347.

Van Aken, G. (2001). Aeration of emulsions by whipping. *Colloids and Surfaces A: Physicochemical and Engineering Aspects, 190*, 333–354.

Vial, Ch., Thakur, R. K., Djelveh, G., & Picgirard, L. (2006). Continuous manufacturing of a light-textured foamed fresh cheese by dispersion of a gas phase. I. Influence of process parameters. *Journal of Food Engineering, 77*, 1–13.

Vial, Ch., Thakur, R. K., Pérez Quintáns, A., Djelveh, G., & Picgirard, L. (2006). Continuous manufacturing of a light-textured foamed fresh cheese by dispersion of a gas phase. II. Influence of formulation. *Journal of Food Engineering, 77*, 14–26.